Effect of HNO_3 and Cl^- on Corrosion Behaviour of AISI 304 and Cr-Mn Austenitic Stainless Steels

Nilay N. Khobragade, Research Scholar, Department of Metallurgical Engineering, Government College of Engineering, Amravati, India 444604
Awanikumar P. Patil, Professor, Department of Metallurgical and Materials Engineering, Visvesvaraya National Institute of Technology, Nagpur, India 440010

Summary

Due to rising cost of Ni, there is interest in low cost Ni-free (Cr-Mn) austenitic stainless steels vis-à-vis AISI 304 (SS304) for a few industrial applications. The present work deals with studying effect of HNO_3/Cl^- ratio on corrosion behaviour of Cr-Mn austenitic stainless steel (Cr-Mn ASS) in comparison with that of SS304. Test methods used were potentiodynamic polarisation (PDP), electrochemical impedance spectroscopy (EIS) and Mott-Schottky analysis. Test solutions were 1000 ppm Cl^-, 0.01M HNO3+1000 ppm Cl^-, 0.1M HNO_3+1000 ppm Cl^- and 1M HNO_3+ 1000 ppm Cl^-. From PDP plots it was found that SS304 exhibited active corrosion in 1000 ppm Cl^- and 0.01M HNO_3+1000 ppm Cl^- solutions, and passivity in 0.1M HNO_3+1000 ppm Cl^- and 1M HNO_3+ 1000 ppm Cl^-. Cr-Mn ASS exhibited active corrosion in 1000 ppm Cl^- and passivity in HNO_3 containing test solutions. From EIS results it was found that polarisation resistance (Rp) decreased on addition of HNO_3 for the both the steels. This is attributed to effect of pH on stability of Cr_2O_3 film. The film of Cr_2O_3 is a p-type semiconductor and has vacancies in cation sub-lattice. When Cl^- is incorporated in anion sub-lattice in sets in Schottky pair reaction by which anion vacancies are created. These vacancies allow migration of cations from metal-film interface to film-solution interface and anions in reverse direction by vacancy aided diffusion process. Therefore, the film forming on test alloys were characterised by Mott-Schottky analysis to find out cation and anion defect densities of passivating film in 1000 ppm Cl^- and 0.1M HNO_3+1000 ppm Cl^- solutions. It was found that density of the cation vacancies in the film forming on SS304 and Cr-Mn ASS in 1000 ppm Cl^- solution was $7.95x10^{20}$ per cm^3 and 12.6 $x10^{20}$ per cm^3, respectively and increased to 78.1 $x10^{20}$ per cm^3 and 87.5 $x10^{20}$ per cm^3 on addition of HNO_3. This explains the role of HNO_3 addition. It was also found that the density of oxygen (anion) vacancies for both the test steels was almost same (approximately $13x10^{20}$ per cm^3) in 1000 ppm Cl^- solution and increased to $18.2x10^{20}$ per cm^3 for SS304 and $29.6x10^{20}$ per cm^3 for Cr-Mn ASS. The rise in defect densities is attributed to drop in pH on addition of HNO_3.

1 Introduction

AISI 304 stainless steel (304 SS) is standard construction material for many industrial applications owing to its excellent corrosion resistance, mechanical strength and good weldability [1]. However, due to rising costs of Ni, interest in low-Ni or Ni-free austenitic stainless steels (Cr-Mn ASS) is increasing [2]. These steels in general are termed as 200 series ASS and account for more than 10% of total stainless steel production [3]. It is expected that their demand would grow with rising cost of Ni. However, due to various

reasons, properties of these grades are inferior to well established grades of 300 series. For example, in absence of Ni, austenitic structure is ensured by 6-10% Mn together with N and/or Cu in 200 series grades or Ni-free Cr-Mn grades [4]. But reducing Ni, limits the maximum Cr-content possible in the alloy and therefore, Cr-content of the 200-series alloys is lower than 300 series alloys. The stainless steels accrue their excellent corrosion resistance primarily from a thin and compact film of Cr_2O_3, which passivates these alloys [1]. Extent of passivation depends upon Cr content and therefore, SS alloys with relatively lower Cr-content will naturally, have lower corrosion resistance. Secondly, Ni not only increases formability, weldability and toughness, but also improves corrosion resistance [5]. It is well known that N addition helps improving corrosion resistance of stainless steel alloys [6]. However, there have been cases of false claim about chemical composition of Cr-Mn ASS. Therefore, chemical composition of 200 grades or Ni-free Cr-Mn steels is suspected and it is recommended that such steels are sourced from highly reputable and informed suppliers [3]. However, when there is increasing pressure to cut cost, it is natural to develop proprietary Cr-Mn SS alloys, not covered by standard chemical specifications. All such new grades obviously have not yet been studied for their corrosion behaviour. Since Ni reserves are rather limited, it is important to investigate performance of Ni-free Cr-Mn ASS thoroughly. So that the end users have sufficient information about properties of newer stainless steels in general and Ni-free/ low Ni Cr-Mn alloys in particular.

2 Experimental Work

The present investigation involves the study of two types of austenitic stainless steels (ASSs) viz. AISI 304 SS and Chrome-Manganese austenitic stainless steel (Cr-Mn ASS). Cr-Mn ASS and AISI 304 SS were procured in the form of sheets (3 mm thick). Specimens of 10 mm x 10 mm size were cut by using electrolytic discharge cutting machine (EDM) from these sheets. Initially to homogenize the microstructure, specimens were solution annealed in silicon carbide muffle furnace at $1050^0C \pm 1^0C$ for one hour and then quenched in water. Chemical composition of these steels is given in Table 1.

Table 1: Chemical composition of studied austenitic stainless steels in weight %.

Elements / Steels	C	Cr	Ni	Mn	Si	P	S	Fe
AISI 304 SS	0.054	20.01	7.97	1.11	0.510	0.0281	0.0061	Bal.
Cr-Mn ASS	0.11	15.86	0.31	9.60	0.434	0.0678	0.0041	Bal.

For electrochemical tests, a piece of copper strip (0.8 mm X 0.8 mm X 3 mm) was soldered with single strand insulated copper wire (18 gauge), then the copper strip was pasted by conducting silver paste on SS specimen and then mounted in araldite to embed the soldered joint leaving other face of the specimen open. The open face of specimen was then abraded on series of emery paper (120-800 grit) and then polished on a cloth smeared with 0.75 µm alumina. The specimens were ultrasonically cleaned after every stage and then used in tests.

Electrochemical tests were carried out in standard 3-electrode system contained in 600 ml four-neck round bottom corning flask; saturated calomel electrode (SCE) was reference electrode and cylindrical platinum gauze electrode was counter electrode. A computer controlled Potentiostat (VersaSTAT 3 of EG&G PAR) was used in conjunction with its V3-Studio software (Princeton Applied Research). After setting up the cell, the specimens were subjected to cathodic cleaning at -1V (SCE) for 1 minute, then left to achieve stable open circuit potential (OCP) for 30 minutes. Then EIS experiment was conducted by using a sinusoidal AC signal of 10 mV in a frequency range of 10^5 to 10^{-2} Hz at open circuit potential. These experiments were controlled by standard V3 Studio software. The EIS data was then used to find out film resistance in various test solutions and values are presented in tabular form. Soon after EIS test was over, polarization test was started from a cathodic potential (OCP minus 300 mV (SCE) and continued up to an anodic potential of 1.5V (SCE). The polarization experiment was carried out at the scan rate of 10mV/min. Electrochemical tests were conducted for triplicate specimens in each experimental condition and all the results obtained were reproducible. Polarization plots were then used to get various electrochemical data. Tafel slopes βa (mV) and βc (mV) and the i_{corr} (μA/cm^2) and were obtained by employing Tafel extrapolation on anodic and cathodic parts of these plots simultaneously using CorrView (Version 2.9) software (Scribner Associates Inc.). The results were then plotted in the form of E- log (i) plots.

Mott-Schottky (M-S) analysis was performed by measuring capacitance immediately after EIS measurements. The capacitance measurements were made on specimens to understand the semiconducting property of the passive film. The polarization cell was used with platinum mesh as a counter electrode and saturated calomel as a reference electrode. VersaSTAT 3 (PAR) FRA was used for these measurements. The M-S analysis was carried out on films formed in two environments given in Table 2. For M-S analysis specimens were exposed for four hours to the solution prior to capacitance was measured at OCP. M-S analysis was carried out in two electrolytes given below.

Table 2: Electrolytes for Mott-Schottky analysis.

Sl. No.	Concentration of solution	Cl^- concentration , ppm
2	DD water	1000
3	0.1 M HNO_3	1000

The capacitive measurements were carried out at a constant frequency of 1000 Hz at 10 mV amplitude voltage as a function of applied potential by potentiodynamic sweeping from -1.5 (SCE) to +1.5V (SCE) at a sweep rate of 10 mV/s. The capacitance (C) was calculated using the Eq.1,

$$C = -\frac{1}{2\pi f Z''} \qquad (1)$$

Where Z" is the imaginary part of the impedance frequency and f is the frequency. From the 'C' values, $1/C^2$ was calculated and was plotted against applied potential. From the

slope *Nd* (donor defect density) and *Na* (acceptor defect density) were calculated using the following equation 2 and 3, respectively:

$$\frac{1}{C^2} = \frac{2}{e\varepsilon\varepsilon_0(Nd)}\left[E - E_{FB} - \frac{kT}{e}\right] \qquad \text{n-type semiconductor} \qquad (2)$$

$$\frac{1}{C^2} = -\frac{2}{e\varepsilon\varepsilon_0(Na)}\left[E - E_{FB} - \frac{kT}{e}\right] \qquad \text{p-type semiconductor} \qquad (3)$$

where, *Nd* is donor defect density, *Na* is acceptor defect density, ε is dielectric constant of passive film, ε_0 is the permittivity of free space ($8.854*10^{-14}$ F/cm), e is the electron charge ($1.602*10^{-19}$ C), k is Boltzmann constant ($1.39*10^{-23}$ J/K), E_{FB} is flat band potential and E is applied potential.

3 Results and Discussion:

Figure 1(a) shows the effect of HNO_3 concentration in the presence of 1000 ppm Cl^- on anodic polarization plots of 304 SS. The plots show that cathodic parts are linear, indicating cathodic reaction to be under activation control. Further, it is evident that in bare chloride solution, active corrosion region extends up to 1 mA c.d. and then a limiting current region sets in. In 0.1M and 1M HNO_3+Cl^- solution the polarization plots show distinct active to passive transition with i_{pass} being more than 1µA. In both the solutions breakdown occurs after 0.75V (SCE). In 0.01M solution secondary passivity is seen. In 0.01M HNO_3+Cl^- solution, it shows active dissolution and the anodic c.d. increases slowly up to 40 µA at 0.75 V(SCE) just before break down. Figure 1(b) shows the effect of HNO_3 concentration in the presence of 1000 ppm Cl^- on anodic polarization of Cr-Mn SS. The plots show that cathodic parts are linear, indicating cathodic reaction to be under activation control. Further, it is evident that in bare chloride solution, active corrosion region extends up to 1 mA c.d. and then a limiting current region sets in. In all HNO_3+Cl^- solutions the polarization plots show distinct active to passive transition with i_{pass} being more than 1µA. In all these solutions film breakdown occurs after 0.75V (SCE) and then a secondary passivity is also seen. Table 3 presents the electrochemical parameters obtained from Figure 1(a) and Figure 1(b). It is evident that i_{corr} of 304 SS in 1000 ppm Cl^- solution is 1.47 µA as against 0.08 µA in distilled water. Similarly, i_{corr} of Cr-Mn SS in 1000 ppm Cl^- solution is 3.28 µA as against 0.76 µA in distilled water. It means that the addition of 1000 ppm Cl^- has adverse effect on both the steels. It is also evident that for 304 SS on addition of 0.1M HNO_3 the i_{corr} decreases to 0.41 µA. It means that in presence of 1000ppm Cl^-, addition of 0.01M HNO_3 is beneficial. Except for this condition, in the presence of 1000 ppm Cl^- the addition of HNO_3 is not beneficial.

Table 4 presents EIS fitted values of test steels measured under OCP (vs. SCE). It is evident that Rp value for 304SS and Cr-Mn SS is 109 and 3.19 kohm-cm^2, respectively in 1000 ppm Cl^- solution as against 608.5 kohm-cm^2 in DD water. The Rp values decrease further with increasing HNO_3 concentration. For both the test steels, Cl^- and

HNO_3 addition has an adverse effect. This may be attributed to the effect of pH; which increases solubility of passivating film.

Table 3: Electrochemical parameters of test steels obtained from anodic polarization in various HNO_3 concentrations containing 1000 ppm Cl^-.

HNO_3 concentration (ppm)	1000 ppm Cl^-		0.01M HNO_3 +1000 ppm Cl^-		0.1M HNO_3 +1000 ppm Cl^-		1M HNO_3 +1000 ppm Cl^-	
Type of steel (ASS)	304	Cr-Mn	304	Cr-Mn	304	Cr-Mn	304	Cr-Mn
E_{corr},V(SCE)	-0.05	-0.15	-0.68	-0.31	-0.209	-0.34	-0.177	-0.40
ßa,(mV)	83.87	112.56	564.5	1.8E7	177.7	1.3E7	66.40	3.0E7
ßc,(mV)	251.33	222.38	80.4	90.75	60.91	103.6	40.44	221.64
i_{corr}, (µA)	**1.47**	3.28	**1.68**	132.8	**0.41**	223.4	**2.74**	15.96
E_{pp}, V(SCE)	-	-		-0.19	0.143	-0.15	-0.13	-0.32
i_{crit}, (µA)	-	-		122.1	22.05	325.2	2.77	14100
i_{pass}, (µA)	-	-		4.22	0.935	9.76	1.48	43.1
E_{pit},V(SCE)	-	-	1.107	0.8	0.806	0.86	0.89	0.91
E_{pit}-E_{pass}, V(SCE)	-	-		0.99	0.66	1.01	1.02	1.23

Table 4: EIS fitted values of test steels measured under OCP (vs. SCE) in solutions containing various HNO_3concentration containing 1000 ppm Cl^-.

HNO_3 concentration, M	Cl^- free		0.01M HNO_3 +1000 ppm Cl^-		0.1M HNO_3 +1000 ppm Cl^-		1M HNO_3 +1000 ppm Cl^-	
Type of steel (ASS)	304	Cr-Mn	304	Cr-Mn	304	Cr-Mn	304	Cr-Mn
Rp, (k ohm-cm^2)	**109.04**	3.19	**1.68**	1.80	**2.15**	0.09	**20.25**	0.001
CPE-*T* (µF-cm^{-2})	42.71	83.47	258.39	269.7	108.7	429.33	92.82	571.2
CPE-*P*	0.85	0.79	0.79	0.78	0.84	0.69	0.87	0.84
Rs, (ohm-cm^2)	10.61	8.33	24.57	24.47	7.77	6.99	4.91	1.42

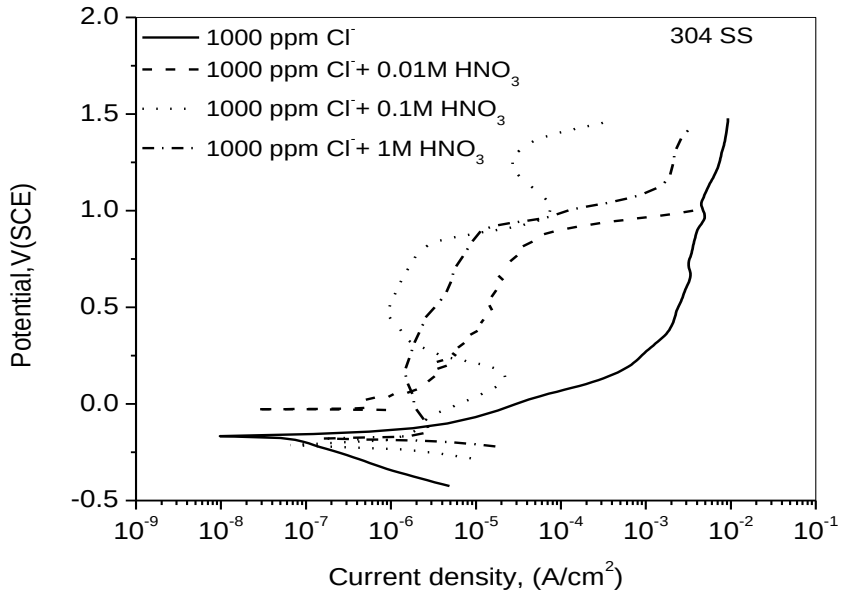

Figure. 1(a): Effect of various concentrations of HNO_3 on anodic polarization of 304 SS in the presence of 1000 ppm Cl^-.

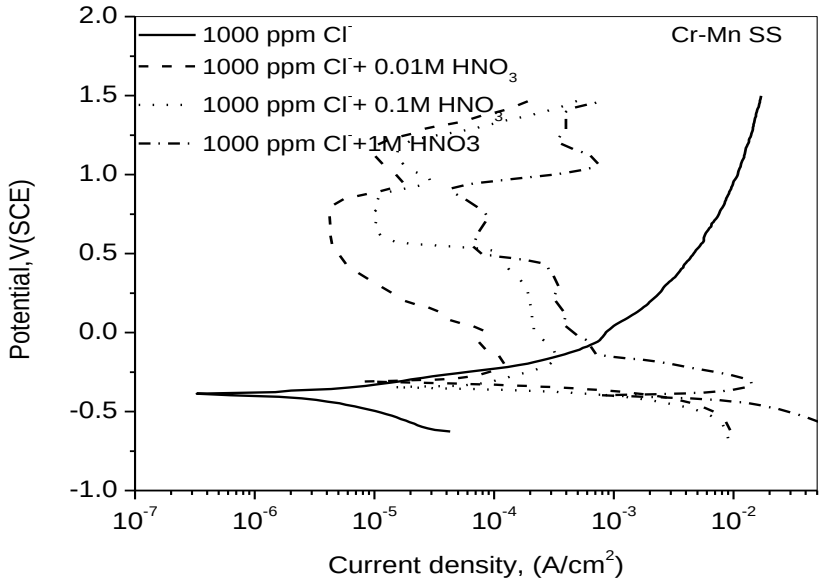

Figure. 1 (b): Effect of various concentrations of HNO_3 on anodic polarization of Cr-Mn SS in the presence of 1000 ppm Cl^-.

It is reported that a process of crevice repassivation mainly depends on the ratio of NO_3^-/Cl^- rather than on individual concentration of NO_3^- or Cl^- ions [7]. Increasing ratio of NO_3^-/Cl^- decreases passivation potential and it causes early passivation [8]. To inhibit pitting corrosion in SS, a ratio of 0.1 of NO_3^-/Cl^- is required in 10% $FeCl_3$ solution. On the other hand, a ratio of 0.067 of NO_3^-/Cl^- is adequate in 1N NaCl + 0.5HCl acidic chloride solution [7]. The ratio of 0.2 of NO_3^-/Cl^- in nitrate and chloride

solution develops crevice resistance in alloy-22 [9]. Yang et al (2007) [10] have observed that the critical breakdown potential varies linearly with log [Cl^-] for solution containing only Cl^- and varies with log ([Cl^-]/[NO_3^-]) for solutions containing $Cl^-$and NO_3^- ions. It means that a particular ratio of NO_3^-/Cl^- only leads to corrosion resistance of an alloy. This result can be explained by the role of NO_3^-/Cl^- ratio on the corrosion behaviour of 304 SS.

Figure 2(a) and 2(b) shows the M-S plots of 304 SS and Cr-Mn SS in DD water containing 1000 ppm Cl^- respectively. The plot for 304 SS and Cr-Mn SS shows two linear regions on either side of minima. These plots are similar to those reported previously for passive films on stainless steels [11]. It reflects duplex nature of the passive film; the inner chromium oxide (Cr_2O_3) region and outer iron oxide (Fe_2O_3) regions of passive films of stainless steels. It is evident that 304 SS has negative slope up till 0.44V (SCE) and shows positive slope from 0.44V (SCE) to 0.86V (SCE). The potential 0.44V (SCE) corresponds to EFB of 304 SS. Also, in Cr-Mn SS a negative slope is observed up till 0.347 V (SCE) and indicates a positive slope from 0.347V (SCE) to 0.86V (SCE). Potential of 0.347 V (SCE) indicates EFB of Cr-Mn SS. It is evident that EFB is lower in Cr-Mn SS. It is likely that lower EFB would yield higher pitting potential [6]. It is evident that in the region of negative slope, the plot of Cr-Mn SS lies above the plot of 304 SS. It means that values of $1/C^2$ for Cr-Mn SS are higher than that of 304 SS. It is also evident that the plot of Cr-Mn SS has lower slope than that of 304 SS. According to finding of Hakiki et al [11], slope of negative plot in M-S plots of Fe-Cr alloys, decreases with increasing Cr content. In the region of positive slope, the plot of Cr-Mn SS lies above that of 304 SS.

It is evident that the slope Cr-Mn SS is lower than the slope of 304 SS. It is evident that the positive slope of Cr-Mn SS is lower than that of 304 SS. This is in agreement with the findings of Hakiki et al [1] that defect density increases with decreasing Cr content of Fe-Cr alloys and that the effect is more clearly seen in negative slope part of M-S plot. This indicates that Cr-Mn SS has more oxygen vacancy in the film than in the film of 304 SS. Less resistant film should have more cation vacancies; this is what has been found in M-S studies that the cation vacancies for 304 SS increases from 7.95 $x10^{20}cm^{-3}$ (in 1000 ppm Cl^-) to 78.1 $x10^{20}cm^{-3}$ on addition of 0.1M HNO_3. Similarly for Cr-Mn SS, *Na* increases from 12.6 $x10^{20}cm^{-3}$ (in 1000 ppm Cl^-) to 87.5 $x10^{20}cm^{-3}$ on addition of 0.1M HNO_3. No doubt that it increases corrosion rate as has been found for both the test steels.

Table 5: Defect density of test steels in various solutions ($10^{20}/cm^3$)

Solution	**304 SS**		Cr-Mn SS	
	Na	*Nd*	*Na*	*Nd*
Distilled water +1000 ppm Cl^-	7.95	13.4	12.6	13.7
0.1M HNO_3 + 1000 ppm Cl^-	78.1	18.2	87.5	29.6

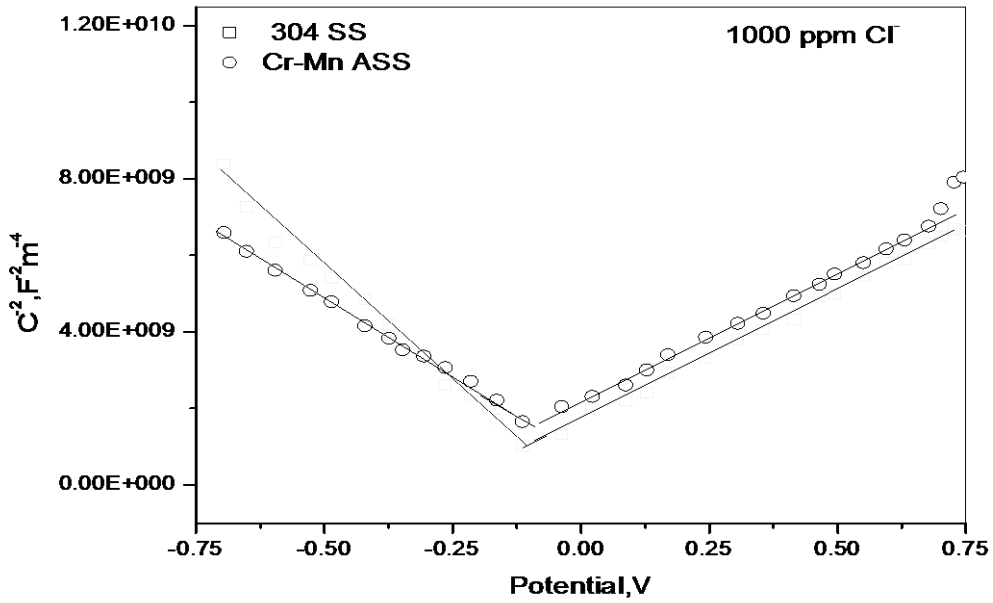

Figure 2(a): M-S plot of 304 SS and Cr-Mn SS in 1000 ppm Cl^- solution.

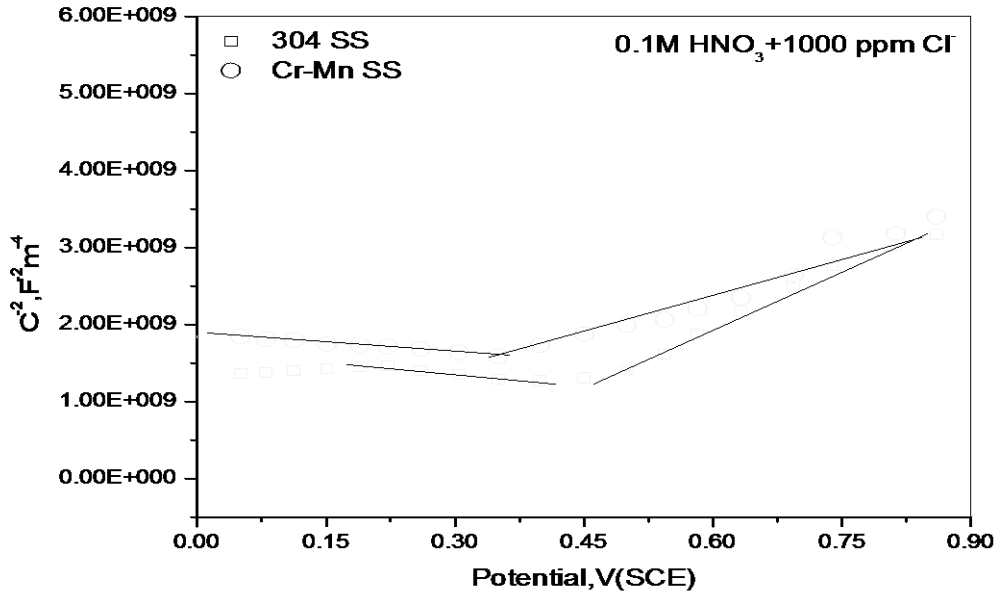

Figure 2(b): M-S plot of 304 SS and Cr-Mn SS in 0.1M HNO_3+1000 ppm Cl^- solution.

4 Conclusions:

(1) It was found that density of the cation vacancies in the film forming on SS304 and Cr-Mn ASS in 1000 ppm Cl^- solution was $7.95x10^{20}$ per cm^3 and 12.6 $x10^{20}$ per cm^3, respectively and increased to 78.1 $x10^{20}$ per cm^3 and 87.5 $x10^{20}$ per cm^3 on addition of HNO_3.

(2) From EIS results it was found that polarisation resistance (Rp) decreased on addition of HNO_3 for the both the steels. This is attributed to effect of pH on stability of Cr_2O_3 film.

(3) This means that addition of 0.01M and 0.1M HNO_3 increases tendency of 304SS to corrode and that addition of 1M HNO_3 decreases its tendency to corrode in case of 304 SS while addition of 0.01M and 0.1M HNO_3 decreases tendency of Cr-Mn SS to corrode and that addition of 1M HNO_3 increases its tendency to corrode in case of Cr-Mn SS.

(4) i_{corr} of 304 SS in 1000 ppm Cl^- solution is 1.47 µA as against 0.08 µA in distilled water. Similarly, i_{corr} of Cr-Mn SS in 1000 ppm Cl^- solution is 3.28 µA as against 0.76 µA in distilled water. It means that the addition of 1000 ppm Cl^- has adverse effect on both the steels.

(5) Except 0.1M of HNO_3 in 304 SS in the presence of 1000 ppm Cl^-, the addition of HNO_3 is not beneficial.

References

[1] A. J. Sedrik, *Corrosion of Stainless Steels, 2 nd ed., John Wiley & Sons, New York*. 1996.

[2] T. Oshima, Y. Habara, and K. Kuroda, “Efforts to Save Nickel in Austenitic Stainless Steels,” *ISIJ International*, vol. 47, no. 3, pp. 359–364, 2007.

[3] ISSF, Brussels, “‘ New 200-series ’ steels : An opportunity or a threat to the image of stainless steel,” no. November, 2005.

[4] P. C. Pistorius and M. Toit, “Low-nickel austenitic stainless steels : metallurgical constraints,” in *The Twelth International Ferroalloys Congress; Sustainable Future*, 2010, pp. 911–918.

[5] C. Abreu, M. Cristobal, R. Losada, X. Novoa, G. Pena, and M. Perez, “The effect of Ni in the electrochemical properties of oxide layers grown on stainless steels,” *Electrochimica Acta*, vol. 51, no. 15, pp. 2991–3000, Apr. 2006.

[6] S. Ningshen, U. Kamachimudali, V. Mittal, and H. Khatak, “Semiconducting and passive film properties of nitrogen-containing type 316LN stainless steels,” *Corrosion Science*, vol. 49, no. 2, pp. 481–496, Feb. 2007.

[7] G. O. Ilevbare, K. J. King, S. R. Gordon, H. a. Elayat, G. E. Gdowski, and T. S. E. Gdowski, “Effect of Nitrate on the Repassivation Potential of Alloy 22 in Chloride-Containing Environments,” *Journal of The Electrochemical Society*, vol. 152, no. 12, p. B547, 2005.

[8] R. C. Newman and M. A. A. Ajjawi, “A micro-electrode study of the nitrate on pitfing of stainless steels,” *Corrosion Science*, vol. 26, no. 12, pp. 1057–1063, 1986.

[9] A. K. Mishra and G. S. Frankel, “Crevice Corrosion Repassivation of Alloy 22 in Aggressive Environments,” *Corosion*, vol. 64, no. 11, pp. 836–844, 2008.

[10] D. D. Macdonald, Shoufeng Yang, “Theoretical and experimental studies of the pitting of type 316L stainless steel in borate buffer solution containing nitrate ion,” *Electrochimica Acta*, vol. 52, pp. 1871–1879, 2007.
[11] N. E. Hakiki, B. Rondot, and S. Boudin, “The electronic formed structure of passive films on stainless steels,” *Corrosion*, vol. 37, no. 11, pp. 1809–1822, 1995.